ELSEVIER

International Journal of Pharmaceutics 191 (1999) 43–50

international journal of pharmaceutics

www.elsevier.com/locate/ijphar

# Interpretation of the differences in the surface energetics of two optical forms of mannitol by inverse gas chromatography and molecular modelling

I.M. Grimsey [a,*], M. Sunkersett [a], J.C. Osborn [a], P. York [a], R.C. Rowe [b]

[a] *Drug Delivery Group, Postgraduate Studies in Pharmaceutical Technology, School of Pharmacy, University of Bradford, Bradford, West Yorkshire, BD7 1DP, UK*

[b] *Zeneca Pharmaceuticals, Alderly Park, Macclesfield, Cheshire, SK10 2NA, UK*

Received 7 April 1999; accepted 3 August 1999

**Abstract**

Inverse gas chromatography (IGC) has been successfully used to characterise the nature of the surface of two optical forms of mannitol, DL and βD. This has shown that the surface energetics of the two forms are significantly different with the DL form having higher values for the interactions with the dispersive and basic probes. Molecular modelling was used to predict the slip planes by utilising attachment energy calculations and so the dominant faces exposed upon milling could be predicted. Imaging these faces showed that the orientation of the molecules at these surfaces differed between the two forms. A visual comparison of the faces indicated that the DL form had a higher density of acidic and dispersive sites exposed at the surfaces than the βD form. The results from the modelling agreed with the trends seen in the changes in surface energetics as measured by IGC. This suggests that the components of the surface energetic terms reflect the density of exposed groups at the particle surfaces. 

*Keywords:* Inverse gas chromatography; Optical forms; Surface free energy; Attachment energies; Fracture planes

## 1. Introduction

For the analysis of surfaces, inverse gas chromatography (IGC) is a very sensitive technique which has been used to demonstrate differences in the properties of pharmaceutical powders (Ticehurst et al., 1994, 1996). It has also recently been shown that the visualisation of the chemical nature of crystal surfaces and the prediction of preferred slip planes, significantly aids the interpretation of IGC data (York et al., 1998). The solid state form of a pharmaceutical material will influence not only its bioavailability and solubility profile but also its processing behaviour.

In this study, the surface energetics of two different optical forms of mannitol have been characterised by inverse gas chromatography. Molecular modelling has been used to investigate

* Corresponding author.

0378-5173/99/$ - see front matter 
PII: S0378-5173(99)00284-7

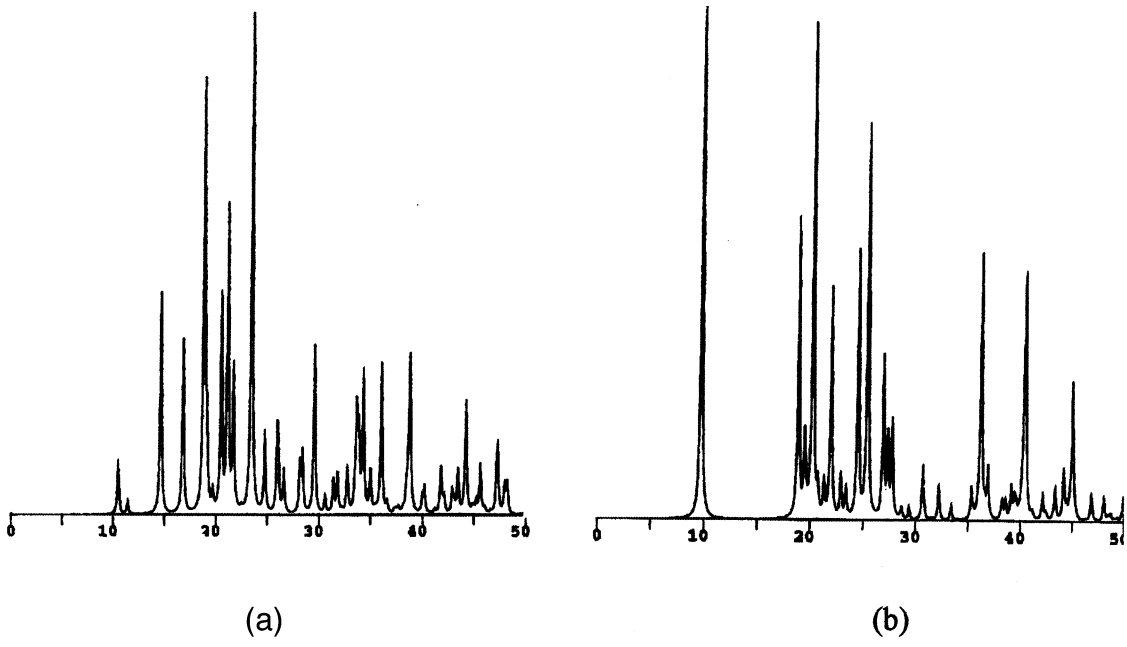


Fig. 1. Theoretical powder X-ray diffraction patterns of (a) βD and (b) DL mannitol generated by Cerius[2].

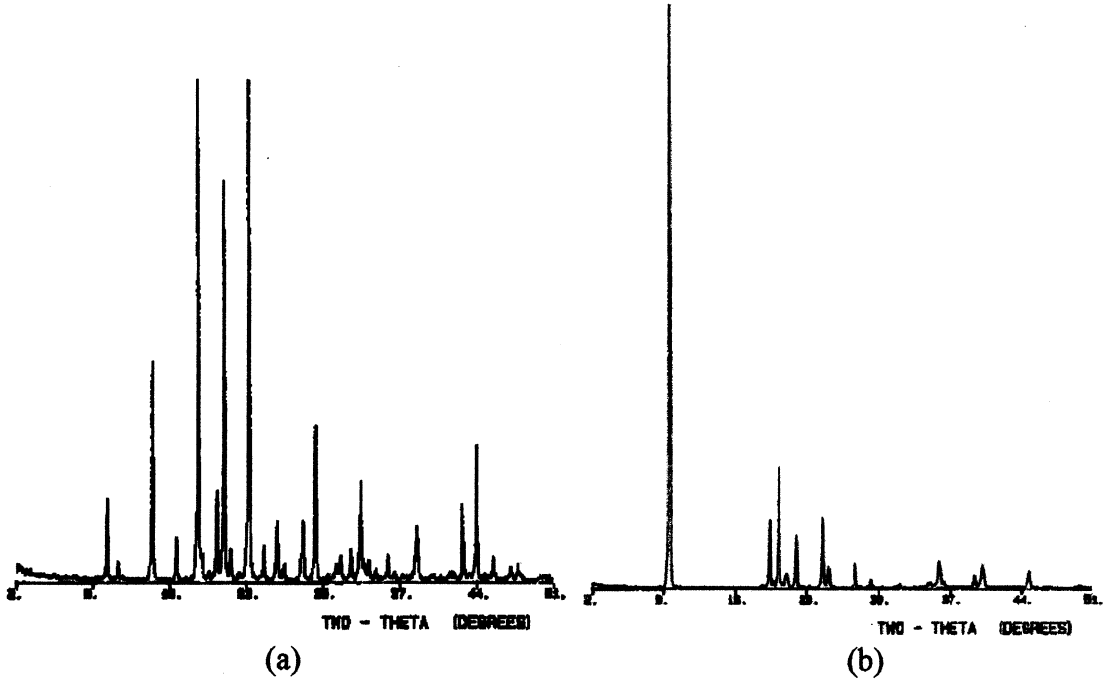


Fig. 2. Experimental powder X-ray diffraction patterns of (a) βD and (b) DL mannitol.

Table 1
Surface energetic parameters for DL and βD mannitol measured by inverse gas chromatography (IGC)

| Sample | $\gamma_S^D$ (mJ m$^{-2}$) | Chloroform | $\Delta G_A^{SP}$ (kJ mol$^{-1}$) Acetone | Tetrahydrofuran |
|---|---|---|---|---|
| DL | 73.3 (2.7) | 0.2 (0.1) | 6.7 (0.1) | 5.4 (0.1) |
| βD | 47.9 (1.7) | 0.7 (0.1) | 4.8 (0.1) | 4.1 (0.1) |

the molecular groups exposed at the surfaces of the two forms and so relate the differences in the surface energetics measured between the two materials to the nature of the surfaces exposed upon milling.

## 2. Materials and methods

### 2.1. Materials

The two batches of mannitol were obtained from BDH Chemicals, Poole, UK, and supplied as ANALAR grade reagents. Probes (HPLC grade) employed for IGC were hexane (Fisons), heptane (Sigma), octane (Aldrich), nonane (Aldrich), tetrahydrofuran (THF) (Rathburn Chemicals) and chloroform (Sigma).

### 2.2. Powder X-ray diffraction

X-ray powder diffraction spectra were taken for each of the samples using a Siemens D5000 over the range 2–50° 2$\theta$ at a scanning rate of 1° (2$\theta$) min$^{-1}$ with a CuKα source ($\lambda = 1.542$ Å).

### 2.3. IGC

Full details of the experimental procedure have been previously published in Ticehurst et al. (1994). Two columns were packed with between 9.5 and 10.7 g of each powder and each column was analysed twice at a column temperature of 30°C. The method of Schultz and Lavielle (1989) was used to determine the dispersive component of the surface free energy ($\gamma_S^D$) and the specific component of the free energy of adsorption ($-\Delta G_A^{SP}$).

### 2.4. Molecular modelling

The single crystal structure of both the DL and βD forms of mannitol were obtained (Berman et al., 1968; Kanters et al., 1977).

Prior to molecular modelling, the hydrogen atom positions in the structures were adjusted to compensate for the imprecision of hydrogen location by X-ray diffraction. In the case of the βD mannitol, some of the experimental bond angles involving hydrogen were found to be unrealistic. Consequently hydrogen atom positions were adjusted to standard bond angles and bond lengths as tabulated by Allen et al. (1987) which were derived from high quality neutron diffraction. For DL mannitol the experimental bond angles were

Table 2
Calculated attachment energies for DL mannitol

| Face (hkl) | Attachment energy (kJ mol$^{-1}$) |
|---|---|
| 002 | −80 |
| 200 | −119 |
| 201 | −142 |
| 203 | −150 |
| 202 | −150 |

Table 3
Calculated attachment energies for βD mannitol

| Face (hkl) | Attachment energy (kJ mol$^{-1}$) |
|---|---|
| 110 | −72 |
| 020 | −75 |
| 120 | −99 |
| 130 | −104 |
| 230 | −126 |

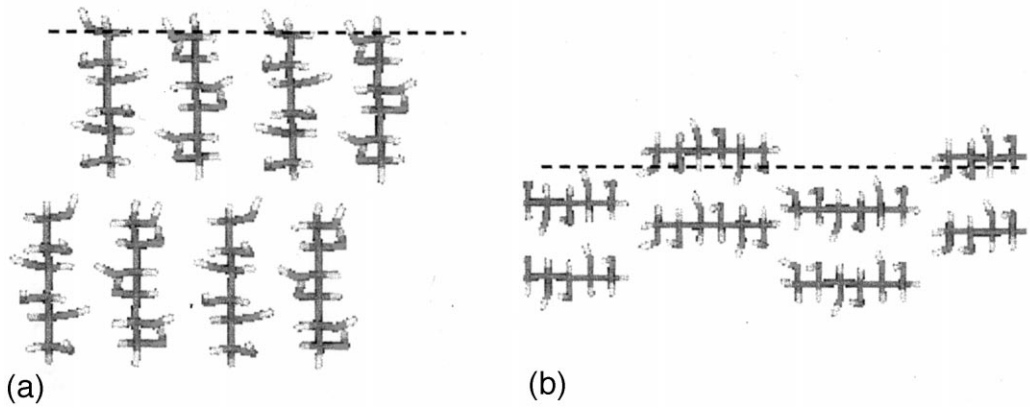


Fig. 3. Slices through the predominant slip planes of DL mannitol. (a) The (002) plane of DL mannitol; (b)the (200) plane of DL mannitol.

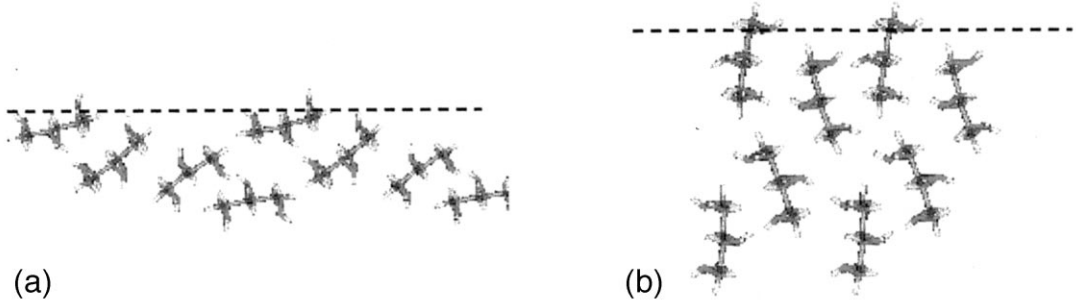


Fig. 4. Slices through the predominant slip planes of βD mannitol. (a) The (110) plane of βD mannitol; (b) the (020) plane of βD mannitol.

reasonable but the bond lengths were normalised to the standard values.

Ab initio molecular orbital calculations at the Hartree–Fock 6-31G** level using the General Atomic and Molecular Electronic Structure System (GAMESS) molecular orbitals package (Schmidt et al., 1993) were used to determine the electrostatic interactions around the isolated molecule. The CHELPG least squares fitting scheme (Breneman and Wiberg, 1990) was applied to assign point charges to each atom, so as to best reproduce the electrostatic potential distribution around the molecule. This distribution is necessary to allow calculation of the electrostatic contribution to the cohesive energy that exists between the individual molecules of the substance in the crystal.

Buckingham (exponential-6) potentials taken from the DREIDING generic force field for molecular modelling (Mayo et al., 1990) were used to model van der Waals type interactions. In addition an anisotropic hydrogen bonding potential from the same force field was applied to the hydrogen bonds between hydroxyl groups.

Electrostatic and van der Waals interactions between molecules whose centres are less than 30 Å apart were taken into account in the energy calculations.

Cerius$^2$ (Version 3.7) (Molecular Simulations, San Diego, CA) was applied to calculate the attachment energies. The slip plane is assigned as the crystal face with the smallest attachment energy. Cerius$^2$ was used to visualise crystal structures, surfaces and predicted morphologies for all

molecules. The software was also used to generate theoretical X-ray diffraction patterns from the single crystal structures, assuming no preferred orientation.

## 3. Results and discussion

The powder X-ray diffraction patterns of the two samples were compared to the theoretical patterns generated using the single crystal data (Figs. 1 and 2). The two powders were identified as the DL and βD forms of mannitol.

Values of the dispersive component of the surface free energy ($\gamma_S^D$) and the specific component of the free energy of adsorption ($-\Delta G_A^{SP}$) for the polar probes are presented in Table 1. The relative basic and acidic nature of the probes can be expressed by the ratio of their Gutmann numbers (DN/AN*) (Gutmann, 1978). THF has a value of 40 and is essentially basic. Chloroform has a value of zero and is therefore acidic. Consequently THF will interact with the acidic sites, and chloroform with the basic sites exposed at the crystal surfaces. The magnitude of both the dispersive interaction and the specific interactions for THF is greater for the DL form of mannitol compared to the Dβ form. The βD form does show a larger interaction with chloroform but in both cases this interaction is small reflecting the essentially acidic nature of mannitol. The acidic sites on mannitol are believed to be the exposed oxygen atoms whilst the dispersive sites are presumed to be the exposed carbon atoms in the chain.

Both powders were investigated by optical microscopy and were observed to consist of fine needle-like particles which would be consistent with the powders having been milled. When a

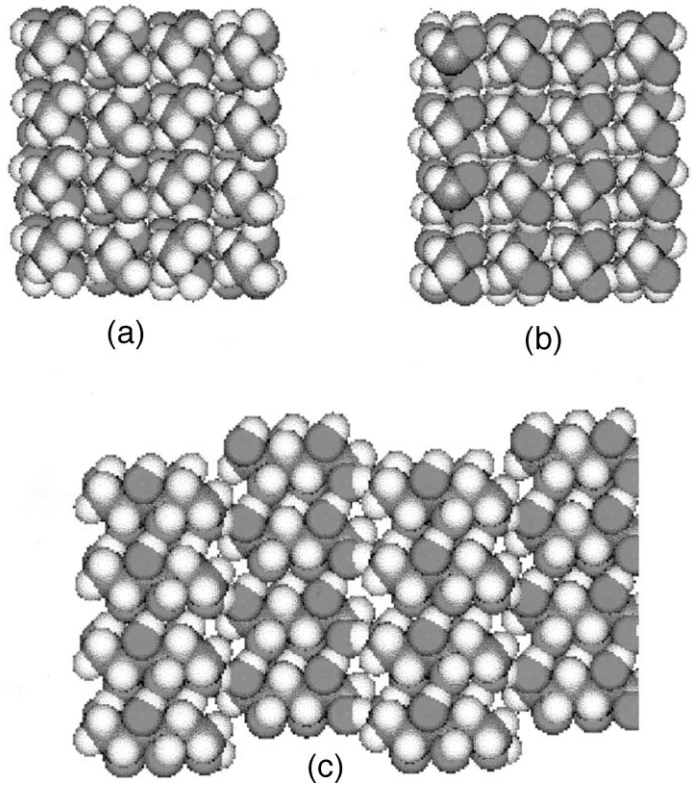


Fig. 5. Molecular arrangement on the predominant faces of DL mannitol. (a) (002) face of DL mannitol; (b) $(00\bar{2})$ face of DL mannitol; (c) (200) and $(\bar{2}00)$ faces of DL mannitol.

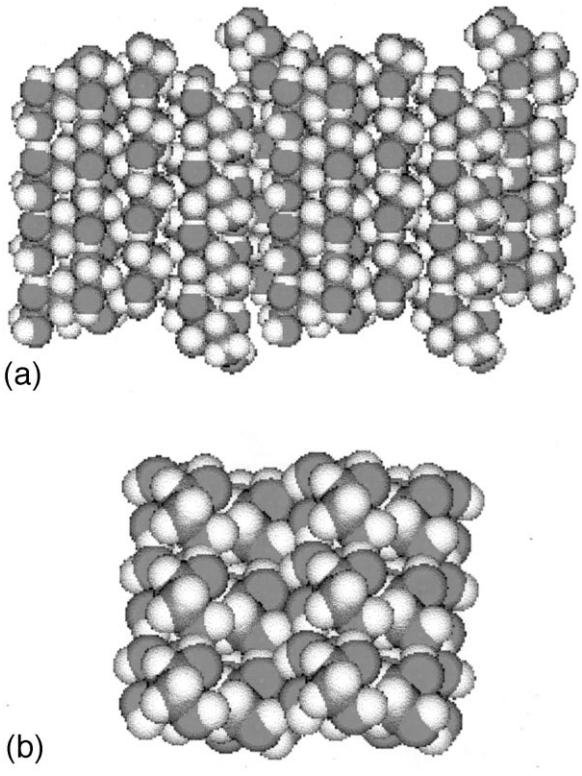


Fig. 6. Molecular arrangement on the predominant faces of Dβ mannitol. (a) (110) and ($\bar{1}\bar{1}$0) faces of βD mannitol; (b) (020) and (0$\bar{2}$0) faces of βD mannitol.

material is milled it is assumed that it will breakdown along the predominant slip planes. The crystals must break along at least two of the slip planes as otherwise the milled particles would appear as platelets. The slip planes in both materials were predicted from the relative attachment energies calculated by the Cerius[2] program. For the DL form the two major slip planes are the (002) and (200) thus producing an increase in the proportions of the (002), (00$\bar{2}$), (200) and ($\bar{2}$00) relative to the rest of the faces on milling (Table 2). In the βD form the two predominant slip planes are the (110) and (020) thus producing an increase in the (110), ($\bar{1}\bar{1}$0), (020) and (0$\bar{2}$0) faces on milling (Table 3).

DL mannitol crystallises in the space group $Pna2_1$ which lacks an inversion centre, which is unusual for a racemic compound. The (002) and the (00$\bar{2}$) faces are inequivalent and must be considered separately. The main difference between them is the orientation of the hydroxyl groups. The (200) and the ($\bar{2}$00) faces are equivalent due to the *n* glide plane and the screw axis. In βD mannitol whose space group is $P2_12_12_1$, (110) is equivalent to ($\bar{1}\bar{1}$0) and (020) is equivalent to (0$\bar{2}$0) due to the screw axis.

A slice view through each plane is shown in Figs. 3 and 4. A surface view of each face is shown in Figs. 5 and 6. The surface area of the unit cell exposed at each surface and a description of the molecular arrangements is given in Table 4.

Initially considering the slip planes for the DL form, it can be seen that on the (002) two molecule ends are exposed, each of which is exposing only one carbon atom. On the opposing (00$\bar{2}$) face each molecule is exposing one oxygen atom and one carbon atom. For the (200) and ($\bar{2}$00) faces there are two molecules of the unit cell exposed. The molecule on the upper layer is exposing one oxygen and four carbon atoms. The

Table 4
The surface area of the unit cell exposed at each surface and a description of the molecular arrangements for DL and βD mannitol

| Crystal form | Surface | Unit cell surface area (Å$^2$) | Comments |
|---|---|---|---|
| DL | (002), (00$\bar{2}$) | 44.1 | Two molecule ends exposed |
| | (200), ($\bar{2}$00) | 88.9 | Two molecule sides exposed of which one is in a trough |
| βD | (110), ($\bar{1}\bar{1}$0) | 105.5 | One molecule side fully exposed and two other molecules partially exposed at an oblique angle in a trough |
| | (020), (0$\bar{2}$0) | 48.2 | Two molecule ends exposed of which one is in a trough |

Table 5
The number and density of acidic and dispersive sites exposed on the faces for the two forms of mannitol

| Crystal form | Surface | No. exposed acidic sites per unit cell surface area | No. exposed dispersive sites per unit cell surface area | Density of acidic sites (Å$^2$) | Density of dispersive sites (Å$^2$) |
|---|---|---|---|---|---|
| DL | (002) | 0 | 2 | 0 | 0.045 |
| | (00$\bar{2}$) | 2 | 2 | 0.045 | 0.045 |
| | (200), ($\bar{2}$00) | 4 | 6 | 0.045 | 0.067 |
| βD | (110), ($\bar{1}\bar{1}$0) | 4 | 5 | 0.040 | 0.047 |
| | (020), (0$\bar{2}$0) | 1 | 1 | 0.021 | 0.021 |

molecule on the lower plane is exposing three oxygen atoms and two carbon atoms.

For the (110) and ($\bar{1}\bar{1}$0) faces on the βD form, three molecules of the unit cell are exposed. Between these molecules, four oxygen atoms and five carbons are exposed.

For the (020) and (0$\bar{2}$0) faces of βD mannitol there are two molecules of the unit cell exposed at the surface in a stepped arrangement. From the slice diagram in Fig. 4b it is suggested that the interaction of any probe with the lower molecule will be restricted and so the interaction on this face will be primarily with the upper molecule. Therefore only one oxygen and one carbon are exposed for the two molecules at the surface.

The density of exposed oxygen and carbons at each surface can be assessed from the exposed number of atoms and the unit cell surface area (Table 5). To determine the density of sites for the crystal as a whole, equal areas of the predominant slip planes for each crystal form are taken and the concentration of the sites on each individual face averaged. From this it can be calculated that for the DL form of mannitol, the average concentration of acidic sites is 0.038 Å$^{-2}$ whilst for the βD form the concentration is 0.031 Å$^{-2}$. This correlates with the higher interaction measured for the THF on the DL form of mannitol. Similarly the average concentration of the dispersive sites for the DL form is calculated to be 0.056 Å$^{-2}$ compared with 0.034 sites Å$^{-2}$ for the βD form. This difference is reflected in the increased dispersive interaction of the alkanes with the DL form.

## 4. Conclusions

By using computational techniques to predict the predominant slip planes and to model their chemical nature, it is suggested that the magnitude of the probe/surface interactions for two chiral forms can linked to the relative exposure of particular atoms at the crystal surfaces.

## Acknowledgements

We acknowledge the Engineering and Physical Sciences Research Council and Zeneca Pharmaceuticals for a CASE studentship for M. Sunkersett in support of this work.

## References

Allen, F.H., Kennerd, O., Watson, D.G., Brammer, L., Orpen, A.G., Taylor, 1987, Tables of bond lengths determined by x-ray and neutron diffraction. Part 1. Bond lengths of organic compounds. J. Chem. Soc. Perkin Trans. II S1

Berman, H.M., Jeffrey, G.A., Rosenstein, R.D., 1968. The crystal structures of the α$^-$ and β forms of D-mannitol. Acta Cryst. B24, 442.

Breneman, C.M., Wiberg, K.B., 1990. Determining atom-centered monopoles from molecular electrostatic potentials — the need for high sampling density in formamide conformational analysis. J. Comp. Chem. 11, 361.

Gutmann, V., 1978. The Donor Acceptor Approach To Molecular Interactions. Plenum, New York.

Kanters, J.A., Roelofien, G., Smits, D., 1977. The crystal and molecular structure of DL mannitol at −150°C. Acta Cryst. B33, 3635–3640.

Mayo, S.L., Olafson, B.D., Goodard, W.A. III, 1990. A generic force field for molecular simulations. J. Phys. Chem. 94, 8897.

Schmidt, M.W., Baldridge, K.K., Boatz, J.A., Elbert, S.T., Gordon, M.S., Jensen, J.H., Koseki, S., Matsunaga, N., Nguyen, K.A., Su, S.J., Windus, T.L., Dupuis, M., Montgomery, J.A., 1993. General atomic and molecular electron-structure system. J. Comp. Chem. 14, 1347.

Schultz, J., Lavielle, L., 1989. Interfacial properties of carbon fibre-epoxy matrix composites. In: Lloyd, D.R., Ward, T.C., Schreiber, H.P. (Eds.), Inverse Gas Chromatography Characterisation of Polymers and Other Materials, ACS Symp. Ser. 391. American Chemical Society, Washington DC, pp. 185–202.

Ticehurst, M.D., Rowe, R.C., York, P., 1994. Determination of the surface properties of two batches of salbutamol sulphate by inverse gas chromatography. Int. J. Pharm. 111, 241–249.

Ticehurst, M.D., York, P., Rowe, R.C., Dwivedi, S.K., 1996. Characterisation of the surface properties of α-lactose monohydrate with inverse gas chromatography, used to detect batch variation. Int. J. Pharm. 141, 93–99.

York, P., Ticehurst, M.D., Osborn, J.C., Roberts, R.J., Rowe, R.C., 1998. Characterisation of the surface energetics of milled DL propranolol hydrochloride using inverse gas chromatography and molecular modelling. Int. J. Pharm. 174, 179–186.